

Article

Determining System Parameters and Target Movement Directions in a Laser Self-Mixing Interferometry Sensor

Bin Liu ^{1,2,*} , Yuxi Ruan ²  and Yanguang Yu ² ¹ School of Physics and Optoelectronics, Xiangtan University, Xiangtan 411105, China² School of Electrical, Computer and Telecommunications Engineering, University of Wollongong, Wollongong, NSW 2522, Australia

* Correspondence: bl987@uowmail.edu.au or liubin816@foxmail.com

Abstract: Self-mixing interferometry (SMI) is a promising sensing technology. As well as its compact structure, self-alignment and low implementation cost, it has an important advantage that conventional two-beam interferometry does not have, i.e., SMI signal fringe evolves into asymmetrical shape with increasing optical feedback level, which leads to discrimination of target movement directions for unambiguous displacement measurement possible by a single-channel interferometric signal. It is usually achieved by using SMI signals in moderate feedback regime, where the signals exhibit hysteresis and discontinuity. However, in some applications, e.g., in biomedical sensing where the target has a low reflectivity, it is hard for the SMI system to operate in a moderate feedback regime. In this work, we present comprehensive analyses on SMI signal waveforms for determining system parameters and movement directions by a single-channel weak feedback SMI signal. We first investigated the influence of two system parameters, i.e., linewidth enhancement factor and optical feedback factor, on the symmetry of SMI signals. Based on the analyses on signal waveform, we then proposed a method of estimating the system parameters and displacement directions. The method was finally verified by experiments. The results are helpful for developing sensing applications based on weak feedback SMI systems.



Citation: Liu, B.; Ruan, Y.; Yu, Y. Determining System Parameters and Target Movement Directions in a Laser Self-Mixing Interferometry Sensor. *Photonics* **2022**, *9*, 612. <https://doi.org/10.3390/photonics9090612>

Received: 12 August 2022

Accepted: 25 August 2022

Published: 29 August 2022

Publisher's Note: MDPI stays neutral with regard to jurisdictional claims in published maps and institutional affiliations.



Copyright: © 2022 by the authors. Licensee MDPI, Basel, Switzerland. This article is an open access article distributed under the terms and conditions of the Creative Commons Attribution (CC BY) license (<https://creativecommons.org/licenses/by/4.0/>).

Keywords: self-mixing interferometry; optical feedback interferometry; linewidth enhancement factor; laser sensor

1. Introduction

Self-mixing interferometry (SMI) has been studied as a promising non-destructive measurement technology in the last several decades for various applications, e.g., measurement of displacement [1], distance [2,3], velocity [4,5], vibration [6,7], material parameters [8], acoustic emission [9], and biomedical signals [10,11]. The sensing mechanism of SMI technology is the self-mixing effect, which occurs when a portion of emitted laser beam is back-reflected by a remote target and is allowed to reenter the laser internal cavity. The back-reflected laser beam carries the information of the external optical path and mixes with the laser beam in the laser cavity, which modulates the laser output power and laser optical frequency in the form of interferometric signals [12,13]. Compared with the conventional two-beam interferometers like Michelson or Mach–Zehnder interferometer, SMI has unique advantages, e.g., the structure is compact, the implementation cost is low, and SMI signals can be collected anywhere the laser beam can reach [12]. More importantly, SMI signals may involve into asymmetrical sawtooth-like shapes with the change of the operation parameters, which makes unambiguous displacement measurement possible using a single interferometric channel [12].

In an SMI sensing system, linewidth enhancement factor (LEF) and optical feedback factor C are important. LEF is also known as α factor or Henry's factor and was first found by Henry in 1982, characterizing many properties of a laser, e.g., the linewidth, the chirp,

and response to optical feedback [14]. Optical feedback factor C influences the operation of a laser [15,16]. Its value discriminates the feedback regime of an SMI system, i.e., weak feedback regime with $C \leq 1$, and moderate/strong feedback regime with $C > 1$ [12]. For SMI-based high-resolution displacement measurement, α and C are often needed, e.g., using phase unwrapping method [17]. As a result, many works have developed various methods to determine the LEF or/and optical feedback factor [18–23].

For SMI-based sensing and measurement, many works have investigated the influences of optical feedback factor on the shape of an SMI signal, and demonstrated that it evolves from being symmetrically sinusoidal to sawtooth-like with increase of C [12,24]. Due to the hysteresis of SMI signals with $C > 1$, unambiguous displacement measurement has been developed [21,25]. Recently, the influence of LEF on shapes of SMI signals has also been explored when $C > 1$ [12,26]. It has been found that directions of the target movement are difficult to determine even when an SMI system is in moderate/strong feedback regime with small LEFs, e.g., in quantum cascade lasers [12]. The work in [26] explored the effect of LEF on the high and low peaks of SMI signals with hysteresis. However, in many practical applications, e.g., biomedical applications [10,11], the reflectivity of the target surface is low, which makes it difficult for the optical feedback factor in such SMI systems to reach values larger than 1. As a result, the behavior of an SMI system in a weak feedback regime is also of significance to analyze. Some works [7,27,28] have already demonstrated that SMI signals show asymmetric shapes with $C \leq 1$, which makes estimation of the target movement direction possible even in weak feedback regime [27]. However, the detailed influence of LEF and noise on the waveform of SMI signals in a weak feedback regime has not been discussed [7,27,28]. Although LEFs of semiconductor lasers often range from 3.0 to 7.0, some other lasers with small LEFs have been also applied for SMI systems, e.g., quantum cascade lasers [12] and solid-state lasers [1,28], since the self-mixing effect is a common phenomenon in lasers regardless of type. Additionally, noises are inevitable in practical applications. Therefore, we discussed the influence of LEF and noise on shape of SMI signals and proposed a simple method to determine LEF, C and displacement directions. The results are useful for designing weak feedback SMI systems for sensing and measurement applications.

2. Theory

2.1. Fundamentals of SMI Theory

A typical SMI system is composed of a laser diode (LD), a photodiode (PD) integrated in the LD package, a lens and a target to be measured [4,9]. Because of the simple structure and low cost, LDs are usually used as the laser sources, but some other types of lasers, e.g., quantum cascade lasers [12], solid-state lasers [1,28], and fiber lasers [2], have also been used in some applications. The widely accepted mathematic model for describing an SMI system is shown as follows [12,24].

$$\phi_F(t) = \phi(t) - C \sin[\phi_F(t) + \arctan\alpha], \tag{1}$$

$$g(t) = \cos[\phi_F(t)], \tag{2}$$

$$P(t) = P_0[1 + m \times g(t)]. \tag{3}$$

where $\phi_F(t)$ and $\phi(t)$ are the optical phases with and without feedback respectively. $\phi(t)$ is expressed as $\phi(t) = 4\pi nL(t)/\lambda_0$, where n is the refractive index of the medium in the external cavity; λ_0 is the laser wavelength of the solitary LD. m is the intensity modulation index with typical values of $\sim 10^{-3}$. $L(t)$ is the external cavity length. When the external target moves, $L(t)$ can be expressed as $L(t) = L_0 + \Delta L(t)$, where L_0 is the initial external cavity length, and $\Delta L(t)$ corresponds to the movement of the target. The optical feedback factor C is defined as [20,24]:

$$C = \eta\kappa\sqrt{1 + \alpha^2\tau/\tau_{in}}, \tag{4}$$

where κ is the feedback strength that is governed by the reflectivity of the laser emitting facet and target surface; η accounts for the coupling efficiency of the re-injection; τ_{in} and τ are the roundtrip time in the internal and external cavity, respectively. For a specific LD, τ_{in} is a constant, and $\tau = 2nL(t)/c$, where c is the light velocity in vacuum. Although C varies with $L(t)$, it is often treated as a constant during the measurement since $\Delta L(t)$ is usually much smaller than L_0 [18]. Although the directly observed signal is the laser output power $P(t)$, $g(t)$ is usually treated as the SMI signal as $g(t)$ can be normalized from $P(t)$ according to Equation (3).

2.2. Symmetry of SMI Signals

As compared with conventional two-beam interferometers, SMI systems have an important advantage that determination of the target movement direction is possible by using a single interferometric channel due to the hysteresis or asymmetry of SMI signals [25,28]. Hysteresis appears when $C > 1$, whereas asymmetry may even appear when $C \leq 1$ [12]. In this work, we mainly investigate the symmetry of SMI signals when $C \leq 1$. Figure 1 presents two typical SMI signals in weak feedback regime with $C = 0.50$ and $\alpha = 5.00$, where Figure 1a is the SMI signal when optical phase increases corresponding to the target moving away from the LD, and Figure 1b is the one when the target moves toward the LD. It can be seen that SMI signal shows clear asymmetry or tilt directions. The SMI signal leans to the right when the target moves away from the LD, whereas it leans to the left when the target moves oppositely.

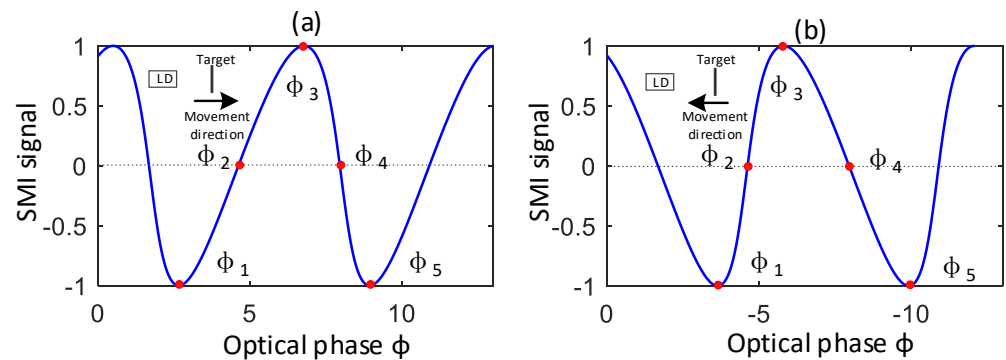


Figure 1. Typical SMI signal (a) when the target moves away from the LD, (b) when the target moves toward the LD.

We pick up some feature points in the SMI signal, i.e., the peak, valley and zero-crossing points, as marked in Figure 1, and denote the corresponding optical phases by ϕ_1 to ϕ_5 . Considering the characteristics of an SMI signal in a weak feedback regime, we introduce a ratio R_{13} to describe the symmetry or tilt direction of an SMI signal, which is defined as $R_{13} = \phi_{13}/\phi_{15}$, where $\phi_{13} = \phi_3 - \phi_1$ and $\phi_{15} = \phi_5 - \phi_1$. For a weak feedback SMI signal, we have $\phi_{15} = 2\pi$ [12]. Thus, we have $R_{13} = \phi_{13}/2\pi$. Then we can describe the symmetry or tilt direction of an SMI signal based on the value of R_{13} . The SMI signal is symmetric or upright with $R_{13} = 50\%$; it is right-tilted with $R_{13} > 50\%$ and is left-tilted with $R_{13} < 50\%$. The farther away R_{13} is from 50%, the more asymmetric an SMI signal is.

Based on the SMI model and mathematic property of trigonometric functions, we can obtain

$$R_{13} = \frac{1}{2} + \frac{\alpha C}{\pi\sqrt{\alpha^2 + 1}} \tag{5a}$$

$$R_{13} = \frac{1}{2} - \frac{\alpha C}{\pi\sqrt{\alpha^2 + 1}} \tag{5b}$$

Here, Equation (5a) is when the target moves away from the LD as in Figure 1a. Equation (5b) is for that as in Figure 1b. It clearly shows that R_{13} can be used to estimate the movement directions. The results of R_{13} are drawn in Figure 2. The SMI signal trends more

to be symmetric when R_{13} is closer to 50% and it is more difficult to use a single-channel SMI signal for determining movement directions when considering the impacts of system noise, sampling frequency of the data acquisition system, etc. It can be seen that R_{13} moves away from 50% with the increase of α and C . For lasers with $\alpha = 0$, e.g., He-Ne lasers, R_{13} is identically equal to 50% with any value of $C \leq 1$. In fact, for such lasers, even when the SMI system is in a moderate feedback regime, it is impossible to distinguish the target displacement directions using a single-channel SMI signal. For lasers with a non-zero LEF, R_{13} never equals to 50%, which means unambiguous measurement are able to be achieved in the whole range of weak feedback regime in theory.

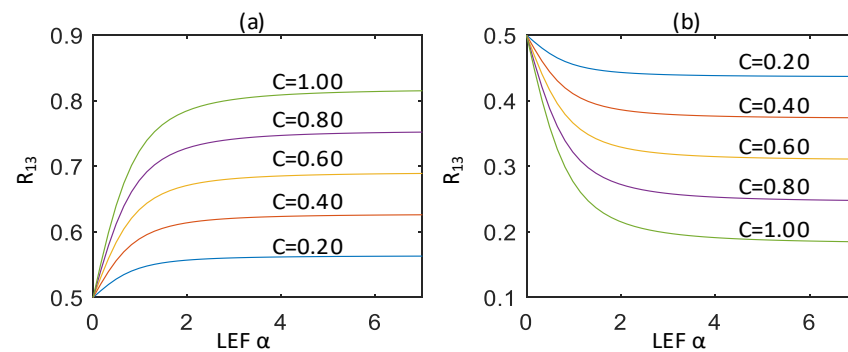


Figure 2. Degree of symmetry of SMI signal with different LEFs and feedback factors, (a) for right-tilted signals, (b) for left-tilted signals.

3. Method and Discussion

3.1. Linear Movement

According to the analyses above, displacement directions of the target can be estimated with the value of R_{13} . The target moves away from the LD with $R_{13} > 50\%$ and it moves toward LD with $R_{13} < 50\%$. Furthermore, based on the values of R_{13} , α and C can also be determined. The measurement principle is presented by taking the right-tilted SMI signal as the example. It is similar for left-tilted SMI signals. As in Figure 1a, we define another ratio, i.e., the ratio of phase difference between two zero-crossing points in a whole SMI fringe, as $R_{24} = \phi_{24} / \phi_{15}$ with $\phi_{24} = \phi_4 - \phi_2$. Then we have:

$$R_{24} = \frac{1}{2} + \frac{C}{\pi\sqrt{\alpha^2 + 1}}. \tag{6}$$

In fact, Equation (6) is also valid for the left-tilted SMI signals. Combining Equations (5) and (6), we get:

$$\alpha = \frac{|R_{13} - 0.5|}{R_{24} - 0.5}. \tag{7}$$

According to Equation (7), α can be calculated once we obtain R_{13} and R_{24} . Then we can calculate C based on Equation (6). In practical fields, we usually get an SMI signal with respect to time as in Figure 3. In this case, R_{13} and R_{24} can be obtained by $R_{13} = t_{13} / t_{15}$ and $R_{24} = t_{24} / t_{15}$, where t_{13} is the time interval between the valley and the adjacent peak points, t_{24} is that between two adjacent zero-crossing points, and t_{15} is the time period of a whole SMI signal fringe when the movement is linear as in Figure 3.

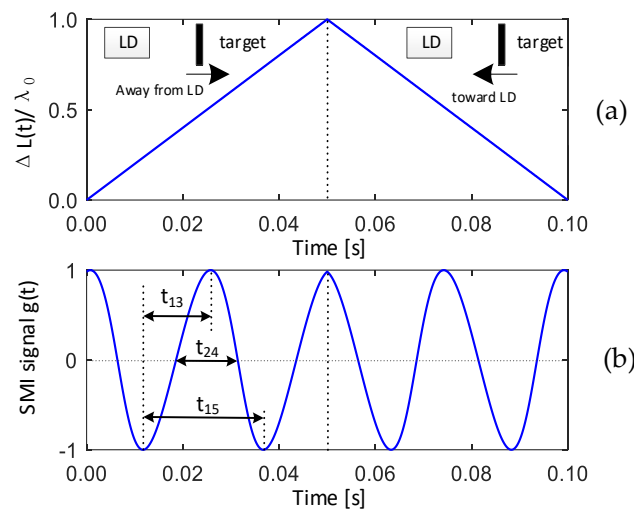


Figure 3. (a) Displacement of the target, (b) the corresponding SMI signal when $C = 0.20$, $\alpha = 5.00$.

3.2. Nonlinear Movement

It is obvious that the movement should be linear when we use the time intervals instead of phase differences to calculate R_{13} and R_{24} . Figure 4 shows an example when the movement is nonlinear with $C = 0.40$ and $\alpha = 3.00$. Thus, R_{13} is 0.621 and 0.379 in theory for the right-tilted and left-tilted fringe, respectively. We choose five different fringes in the SMI signal, i.e., Fringes 1 to 5 in Figure 4 to perform the method. Table 1 shows the final measurement results. We use \hat{R}_{13} , $\hat{\alpha}$ and \hat{C} to denote the estimated values. $\delta_{R_{13}}/R_{13} = |\hat{R}_{13} - R_{13}|/R_{13}$ is the relative error for R_{13} . It is the same for α and C . It can be seen that the estimated results from Fringe 1 have the smallest error. The reason is obvious, in that the displacement corresponding to Fringe 1 has the best linearity. For Fringe 5, the measurement results are almost unreliable with large errors.

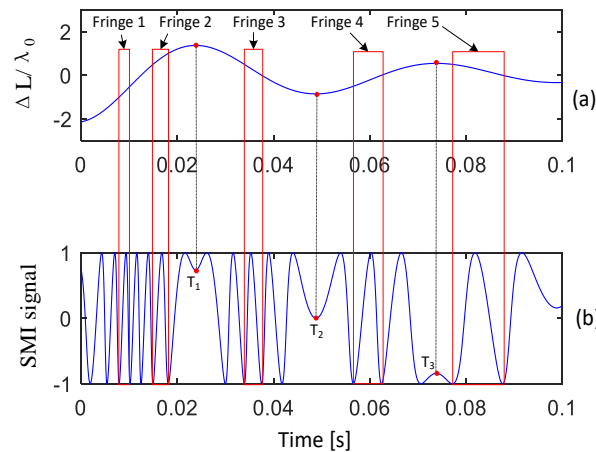


Figure 4. (a) Displacement, (b) the corresponding SMI signal.

Table 1. Measurement results with different fringes.

	\hat{R}_{13}	$\delta_{R_{13}}/R_{13}$	$\hat{\alpha}$	δ_{α}/α	\hat{C}	δ_C/C
Fringe 1	0.625	0.6%	2.91	3.0%	0.42	5.0%
Fringe 2	0.615	1.0%	3.29	8.3%	0.38	5.0%
Fringe 3	0.374	1.3%	2.86	5.0%	0.42	5.0%
Fringe 4	0.635	2.3%	2.70	10.0%	0.45	12.5%
Fringe 5	0.453	20.8%	4.27	42.3%	0.15	62.5%

Therefore, the procedure of determining α , C and displacement direction of nonlinear movement is as follows:

1. Find the fringe corresponding to a displacement with the best linearity. It is obvious that the displacement is with good linearity when there are at least two adjacent fringes with the same or closest values of t_{15} .
2. Use the fringe in step 1 to calculate R_{13} and R_{24} , and further calculate α and C based on Equations (6) and (7).
3. Determine the displacement directions based on R_{13} of the fringe in step 1. This procedure is simple. For a nonlinear movement with several direction-reverse points, we can easily localize them in the corresponding SMI signal, i.e., they are the local but not global maximum or minimum points as T_1 , T_2 and T_3 in Figure 4. The movement direction reverses once when the SMI signal passes a direction-reverse point, e.g., we get $\hat{R}_{13} = 0.625$ for Fringe 1, and thus we can determine the displacement is away from the LD at this point, and it keeps the same until passing T_1 . The remaining directions can be determined by the same way.

Note that the proposed method has limitations. Firstly, displacement should be larger than half laser wavelength. Then, there should be a piece of displacement (at least $\lambda_0/2$) within the whole movement which has relatively good linearity. Otherwise, the estimated results may suffer undesirable errors. However, this problem may be solved by linearly modulating the laser wavelength thanks to the capability of injection current modulation of LDs. Because the displacement is usually much smaller than the initial external cavity length, optical feedback factor can be treated as constant during the measurement. Thus, we can linearly modulate the laser frequency via injection current while keeping the target static. In this way, α and C can also be estimated based on Equations (6) and (7).

3.3. Impact of Noise

In practical applications, SMI signals often suffer impacts of noise from different sources, e.g., the laser itself, the measurement ambience and electronic components. We first analyzed the influence of noise on discrimination of movement directions. For a given α , it was conducted by the following procedure as shown in Figure 5.

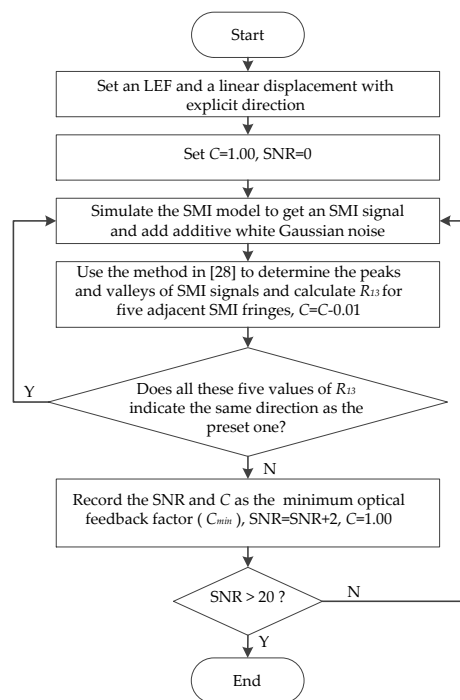


Figure 5. Flow chart of determining the required minimum C for different SNRs with a given α .

Changing the value of α and repeating the procedure in Figure 5, we can get the simulation results for different LEFs as shown in Figure 6. It can be seen that C_{min} decreases with the increase of SNR. For a given SNR, the smaller the LEF is, the larger the required C_{min} is. When SNR is relatively large, C_{min} for different LEFs are close to a constant when LEF is relatively large, e.g., C_{min} is about 0.1 with SNR = 20 dB when LEFs is 3.0, 5.0 and 7.0, which are the commonest values for commercial LDs. However, the required C_{min} is still larger than 0.2 for $\alpha = 0.5$. C_{min} increases rapidly when SNR decreases. Particularly, it increases faster with a smaller LEF, which means C_{min} is more sensitive to the noise for an SMI system with a laser with a small LEF, e.g., quantum cascade lasers [12], or solid-state lasers [28]. Thus, the larger the LEF is, the smaller the feedback factor allowed. Figure 6 is an example for the variation trend of C_{min} with LEF and SNR by taking the method in [28] to obtain R_{13} . If R_{13} is determined more precisely, the curves in Figure 6 may move downwards overall, which means an SMI signal with feedback factor smaller than 0.10 may be used for determining the movement directions.

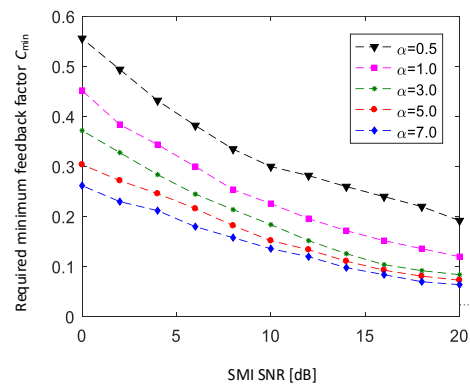


Figure 6. Required minimum C for different LEFs and SNRs.

We then discussed the influence of noise on the accuracy of the proposed method for estimating α and C. We took the SMI signal in Figure 3 as the example and added different levels of noise; Table 2 shows the results. It can be seen that a relatively high accuracy can be achieved with an SNR larger than 20 dB.

Table 2. Impact of noise on the proposed method.

SNR (dB)	Estimated α	Relative Error	Estimated C	Relative Error
5	5.66	13.2%	0.23	15.0%
15	4.68	6.4%	0.18	10.0%
20	4.90	2.0%	0.19	5.0%

4. Experiment

An experimental setup was built as in Figure 7. Two commercial TO-Can packaged near-infrared single mode LDs (Sanyo, DL4140-001S; Hitachi, HL8325G) were tested. A current and temperature LD controller (Thorlabs, ITC4001) is used to drive the lasers. The optical feedback strength is adjusted by a variable attenuator (VA) (Thorlabs, NDC-50C-2M-B). A piezoelectric transducer (PZT) (Thorlabs, PAS005) with a mirror affixed on the surface is assembled on a linear translation stage, which acts as the external target. Displacements are generated by controlling the PZT driver (Thorlabs, MDT694). The integrated PD is used to detect the optical SMI signals, which is followed by a detection circuit. Finally, we use a digital oscilloscope (OSC) to capture and store SMI signals.

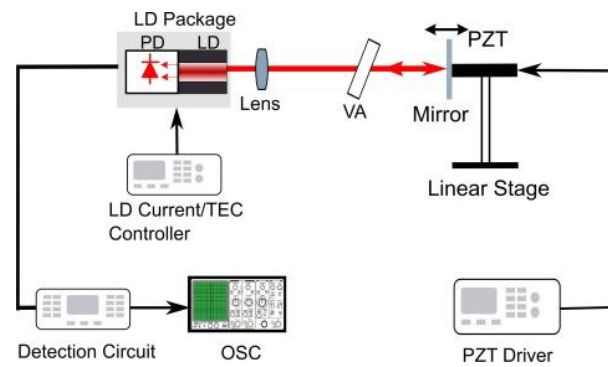


Figure 7. Experimental setup.

The LD operating temperature was stabilized at $T = 23 \pm 0.01 \text{ }^\circ\text{C}$ by using the LD controller. Note that the system has been tested to operate with an initial external cavity length up to 2.5 m and 1.5 m for DL4140-001S and HL8325G, respectively. During the experiments, multi-modality of the LD should be also avoided by adjusting the operation parameters, e.g., the injection current [29]. The sampling rate was set with 100 kHz. Figure 8 is one of the experimental signals for DL4140-001S, from which, we can get $\text{SNR} \approx 21 \text{ dB}$. As a result, the required minimum optical feedback factor for determining the displacement direction is estimated to be approximately 0.10 according to Figure 6.

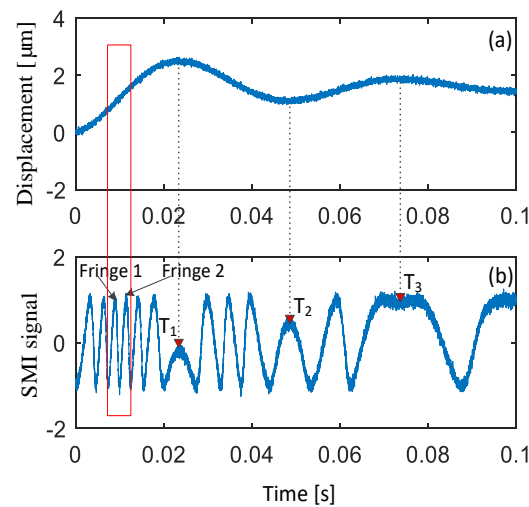


Figure 8. Example of experimental SMI signal, (a) displacement, (b) the corresponding SMI signal.

Based on Figure 8, α and C were estimated by using the proposed method. We found Fringes 1 and 2 correspond to similar linearity. Hence, we used both of them to calculate α and C , and took the average as the results for the signal in Figure 8 with $\hat{R}_{13} = 0.613$, $\hat{\alpha} = 2.70$ and $\hat{C} = 0.38$. Then, the movement direction corresponding to these two fringes is away from the LD since $\hat{R}_{13} > 50\%$. Afterwards, we can easily determine the direction-reverse points in the SMI signal, i.e., T_1 , T_2 and T_3 in Figure 8. Thus, we can say the target moves away from the LD before T_1 point. It moves toward the LD between T_1 and T_2 . After T_2 point, it reverses to move away and reverses again at T_3 point. The estimated displacement directions are coincident with the preset ones. Similarly, we repeat the experiments with HL8325G. We also measured α and C by the method in [19] for comparison. Note that we captured five SMI signals for each LD to calculate α and C and took the average values of all these five measurements as the final results. The results are shown in Table 3, which verifies the proposed method.

Table 3. Estimated LEFs and optical feedback factors for different LDs.

	DL4140-001S		HL8352G	
	$\hat{\epsilon}$	\hat{C}	$\hat{\epsilon}$	\hat{C}
Proposed method	2.73	0.36	3.14	0.21
Method in [19]	2.80	0.41	3.10	0.17

5. Conclusions

The waveform asymmetry of weak feedback SMI signals was discussed for determining the system parameters and movement directions in this work. The influence of LEF and optical feedback factor on the shape of a weak feedback SMI signal was investigated. It was found that an SMI system based on a laser with non-zero LEF is able to achieve unambiguous displacement measurement in the whole range of weak feedback regime in theory. Based on the waveform analyses, we proposed a method to estimate LEF and optical feedback factor and displacement directions, which was verified by experiments. One point that needs to be noted is that there should be a piece of displacement (at least $\lambda_0/2$) within the whole movement which has relatively good linearity when performing the proposed method. The results are helpful for designing weak feedback SMI sensing systems.

Author Contributions: Conceptualization, B.L., Y.R. and Y.Y.; methodology, B.L.; software, B.L. and Y.R.; validation, B.L.; writing—original draft preparation, B.L.; writing—review and editing, B.L., Y.R. and Y.Y.; visualization, B.L.; supervision, B.L. and Y.Y.; project administration, B.L.; funding acquisition, B.L. All authors have read and agreed to the published version of the manuscript.

Funding: This research was funded by the National Natural Science Foundation of China, grant number 62005234, and the Scientific Research Foundation of Hunan Provincial Education Department, grant number 20C1791. The APC was funded by the National Natural Science Foundation of China, grant number 62005234.

Data Availability Statement: The data presented in this study are available on request from the corresponding author. The data are not publicly available since the data also form parts of an ongoing study.

Conflicts of Interest: The authors declare no conflict of interest.

References

- Zhu, K.; Guo, B.; Lu, Y.; Zhang, S.; Tan, Y. Single-spot two-dimensional displacement measurement based on self-mixing interferometry. *Optica* **2017**, *4*, 729–735. [[CrossRef](#)]
- Zhao, Y.; Wang, C.; Zhao, Y.; Zhu, D.; Lu, L. An All-Fiber Self-Mixing Range Finder With Tunable Fiber Ring Cavity Laser Source. *J. Lightwave Technol.* **2021**, *39*, 4217–4224. [[CrossRef](#)]
- Guo, D.; Wang, M. Self-mixing interferometry based on a double-modulation technique for absolute distance measurement. *Appl. Opt.* **2007**, *46*, 1486–1491. [[CrossRef](#)]
- Jiang, C.; Geng, Y.; Liu, Y.; Liu, Y.; Chen, P.; Yin, S. Rotation velocity measurement based on self-mixing interference with a dual-external-cavity single-laser diode. *Appl. Opt.* **2019**, *58*, 604–608. [[CrossRef](#)] [[PubMed](#)]
- Chen, J.; Zhu, H.; Xia, W.; Guo, D.; Hao, H.; Wang, M. Self-mixing birefringent dual-frequency laser Doppler velocimeter. *Opt. Express* **2017**, *25*, 560–572. [[CrossRef](#)] [[PubMed](#)]
- Annovazzi-Lodi, V.; Merlo, S.; Norgia, M. Measurements on a micromachined silicon gyroscope by feedback interferometry. *IEEE ASME Trans. Mechatron.* **2001**, *6*, 1–6. [[CrossRef](#)]
- Zhang, Z.; Jiang, C.; Shen, L.; Li, C.; Huang, Z. Vibration Measurement Based on the Local Maximum Detection Algorithm for Laser Self-Mixing Interferometry. *IEEE Access* **2020**, *8*, 63462–63469. [[CrossRef](#)]
- Wang, B.; Liu, B.; An, L.; Tang, P.; Ji, H.; Mao, Y. Laser Self-Mixing Sensor for Simultaneous Measurement of Young's Modulus and Internal Friction. *Photonics* **2021**, *8*, 550. [[CrossRef](#)]
- Liu, B.; Ruan, Y.; Yu, Y. All-Fiber Laser-Self-Mixing Sensor for Acoustic Emission Measurement. *J. Lightwave Technol.* **2021**, *39*, 4062–4068. [[CrossRef](#)]
- Norgia, M.; Pesatori, A.; Rovati, L. Self-mixing laser Doppler spectra of extracorporeal blood flow: A theoretical and experimental study. *IEEE Sens. J.* **2012**, *12*, 552–557. [[CrossRef](#)]

11. Wei, Y.; Wang, X.; Huang, W.; An, T.; Xu, H. Double-path acquisition of pulse wave transit time and heartbeat using self mixing interferometry. *Opt. Commun.* **2017**, *393*, 178–184. [[CrossRef](#)]
12. Taimre, T.; Nikolić, M.; Bertling, K.; Lim, Y.L.; Bosch, T.; Rakić, A.D. Laser feedback interferometry: A tutorial on the self-mixing effect for coherent sensing. *Adv. Opt. Photonics* **2015**, *7*, 570–631. [[CrossRef](#)]
13. Gao, B.; Qing, C.; Yin, S.; Peng, C.; Jiang, C. Measurement of rotation speed based on double-beam self-mixing speckle interference. *Opt. Lett.* **2018**, *43*, 1531–1533. [[CrossRef](#)] [[PubMed](#)]
14. Henry, C. Theory of the linewidth of semiconductor lasers. *IEEE J. Quantum Electron.* **1982**, *18*, 259–264. [[CrossRef](#)]
15. Acket, G.A.; Lenstra, D.; den Boef, A.; Verbeek, B. The influence of feedback intensity on longitudinal mode properties and optical noise in index-guided semiconductor lasers. *IEEE J. Quantum Electron.* **1984**, *20*, 1163–1169. [[CrossRef](#)]
16. Liu, B.; Jiang, Y.; Ji, H. Sensing by Dynamics of Lasers with External Optical Feedback: A Review. *Photonics* **2022**, *9*, 450. [[CrossRef](#)]
17. Fan, Y.; Yu, Y.; Xi, J.; Chicharo, J.F. Improving the measurement performance for a self-mixing interferometry-based displacement sensing system. *Appl. Opt.* **2011**, *50*, 5064–5072. [[CrossRef](#)]
18. Yu, Y.; Giuliani, G.; Donati, S. Measurement of the linewidth enhancement factor of semiconductor lasers based on the optical feedback self-mixing effect. *IEEE Photonics Technol. Lett.* **2004**, *16*, 990–992. [[CrossRef](#)]
19. Xi, J.; Yu, Y.; Chicharo, J.F.; Bosch, T. Estimating the parameters of semiconductor lasers based on weak optical feedback self-mixing interferometry. *IEEE J. Quantum Electron.* **2005**, *41*, 1058–1064.
20. Khan, J.I.; Zabit, U. Deformation Method of Self-Mixing Laser Sensor's Feedback Phase for Estimation of Optical Feedback Coupling Factor and Displacement. *IEEE Sens. J.* **2021**, *21*, 7490–7497. [[CrossRef](#)]
21. Kim, J.-H.; Kim, C.-H.; Yun, T.-H.; Hong, H.-S.; Ho, K.-M.; Kim, K.-H. Joint estimation of self-mixing interferometry parameters and displacement reconstruction based on local normalization. *Appl. Opt.* **2021**, *60*, 2282–2287. [[CrossRef](#)] [[PubMed](#)]
22. Liu, B.; Ruan, Y.; Yu, Y.; Wang, B.; An, L. Influence of feedback optical phase on the relaxation oscillation frequency of a semiconductor laser and its application. *Opt. Express* **2021**, *29*, 3163–3172. [[CrossRef](#)]
23. An, L.; Liu, B. Measuring parameters of laser self-mixing interferometry sensor based on back propagation neural network. *Opt. Express* **2022**, *30*, 19134–19144. [[CrossRef](#)]
24. Yu, Y.; Xi, J.; Chicharo, J.F.; Bosch, T.M. Optical Feedback Self-Mixing Interferometry with a Large Feedback Factor C: Behavior Studies. *IEEE J. Quantum Electron.* **2009**, *45*, 840–848. [[CrossRef](#)]
25. Bes, C.; Plantier, G.; Bosch, T. Displacement measurements using a self-mixing laser diode under moderate feedback. *IEEE Trans. Instrum. Meas.* **2006**, *55*, 1101–1105. [[CrossRef](#)]
26. Kim, C.; Lee, C.; Kwonhyok, O. Effect of linewidth enhancement factor on fringe in a self-mixing signal and improved estimation of feedback factor in laser diode. *IEEE Access* **2019**, *7*, 28886–28893. [[CrossRef](#)]
27. Merlo, S.; Donati, S. Reconstruction of displacement waveforms with a single-channel laser-diode feedback interferometer. *IEEE J. Quantum Electron.* **1997**, *33*, 527–531. [[CrossRef](#)]
28. Kou, K.; Wang, C.; Lian, T.; Weng, J. Fringe slope discrimination in laser self-mixing interferometry using artificial neural network. *Opt. Lasers Technol.* **2020**, *132*, 106499. [[CrossRef](#)]
29. Usman, M.; Zabit, U.; Bernal, O.D.; Raja, G. Blind identification of occurrence of multi-modality in laser-feedback-based self-mixing sensor. *Chin. Opt. Lett.* **2020**, *18*, 011201. [[CrossRef](#)]